Experimental Quantitative Comparison of Different Control Architectures for Master–Slave Teleoperation

Iñaki Aliaga, Ángel Rubio, and Emilio Sánchez

***Abstract*—A procedure for experimental evaluation and objective/quantitative comparison among the different teleoperation architectures and systems is proposed. It is based on the analysis of the different matrices that can define the teleoperated system (two-port representations) and the selection of a set of four parameters that are easy to estimate via simple experimentation: free motion impedance, position tracking in free movement, force tracking in hard contact tasks and maximum transmittable impedance. These parameters provide complete characterization of the master–slave system and have clear physical interpretation. Furthermore, they require no maneouvering of the slave robot, which is very useful in the case of heavy or nonaccessible industrial robots. The method has been applied to compare position-position (PP), force-position (FP), and four-channel (4C) controllers in a 2 DOF master–slave system. Experimental measuring for all four parameters will be shown, proving the 4C architecture clearly better than any other.**

***Index Terms*—Bilateral control, force feedback, performance comparison, teleoperation.**

I. Introduction

THE aim of a teleoperated system is to enable the operators to undertake precise work in inaccessible or hazardous environments such as radioactive areas in nuclear power stations [1], pressurized underwater zones—for which there are commercially available systems—or even in space on tasks demanded by the aerospace industry [2]. A teleoperated system consists of a set of two robots, referred to as the master robot and the slave robot, together with appropriate sensors and a computer for control architecture implementation purposes. The master robot is that which is directly driven by the operator from his work place, whereas the slave robot is that which is located in the remote environment, ready to follow any trajectories that the operator orders by the movement of the master robot.

While accurate tracking is essential for the skillful control of tasks, it is not enough to achieve really good performance on its own since position is not the only relationship that exists between both robots. In fact, at the moment that the slave robot starts its interaction with the environment, reaction forces appear. Consider the case of a teleoperated drill working in a radioactive area inside a power station. If a hole has to be drilled and the operator has just visual feedback of the operation, he will be able to check how far the drill has penetrated but not to feel the reaction force that the wall exerts on the drill. As a result, he may drive the master robot too quickly, obliging the drill to perforate the surface so rapidly that the increasing reaction forces would break the bit.

Consequently, the feedback of force turns out to be extremely useful and leads to so-called force-reflecting master–slave systems, which not only try to achieve good tracking during unconstrained motion, but also to convey precise information of the forces that appear between the slave robot and the environment, so that the operator can actually feel them on the master robot. Ideally, the operator should feel exactly the same forces he would feel if he were working directly on the remote environment with the tool that is actually at the end effector of the slave robot. In terms of the proposed example, the operator would exert the same force on the master as he would exert on the wall itself if he were handling the drill with his own hands. It is often said that such a system achieves perfect transparency [3]–[5].

In practice, master–slave systems do not provide the operator with perfect transparency, but some control architectures clearly perform better than others. Those differences are easily noticeable for the operator who is working with the system, but, to the knowledge of the authors, an objective procedure of experimental evaluation has not been proposed yet. This paper tries to cover that lack with a set of four parameters that can be obtained through simple tests in a master–slave system: free motion impedance, position tracking in free movement, force tracking in hard contact tasks and maximum transmittable impedance (see Sections II and III for thorough descriptions). These parameters characterize a teleoperated system quantitatively and they support the subjective evaluation of the operator who made the experiments that will be shown. As a result, they constitute a characterization that provides a criterion by which to compare different control architectures.

The analyzed algorithms are position-position (PP) [3], [6]–[8], force-position (FP) [1], [3], [6]–[8] and four-channel (4C) controller algorithms [3], [5]. All three are well known in the literature. However, implementation of the three in a single test-bed has never been reported. The authors have implemented them in a 2 DOF master–slave system and have used the proposed parameters for their comparison. The tuning of the algorithms was made on the basis of the analytical expression of each parameter.

Manuscript received December 12, 2001. Manuscript received in final form May 1, 2003. Recommended by Associate Editor F. Ghorbel. This work was supported by Iberdrola, with which this work has been carried out within the "Simantel" project.

I. Aliaga is with the LANDER Simulation and Training Solutions, S.A., 20018 San Sebastián, Spain (e-mail: ialiaga@landersimulation.com).

Á. Rubio and E. Sánchez are with the Applied Mechanics Department, Centro de Estudios e Investigaciones Técnicas de Gipuzkoa (CEIT), 20018 San Sebastián, Spain (e-mail: arubio@ceit.es; esanchez@ceit.es).

Digital Object Identifier 10.1109/TCST.2003.819586

II. Theoretical Characterization of a Teleoperator

From the mathematical point of view, a teleoperated system is just a relationship between the positions and forces of the two robots, i.e., a set of four signals, namely X_m (position of the master robot), X_s (position of the slave robot), F_m (force applied on the master robot by the operator), and F_s (force exerted on the environment by the slave robot). These signals relate to each other in terms of six different matrices (two-port representations), as shown in (1) to (6).

$$\begin{bmatrix} F_m \\ F_s \end{bmatrix} = [\mathbf{Z}] \cdot \begin{bmatrix} X_m \\ X_s \end{bmatrix} \quad \text{Impedance matrix} \tag{1}$$

$$\begin{bmatrix} X_m \\ X_s \end{bmatrix} = [\mathbf{Y}] \cdot \begin{bmatrix} F_m \\ F_s \end{bmatrix} \quad \text{Admittance matrix} \tag{2}$$

$$\begin{bmatrix} F_m \\ X_s \end{bmatrix} = [\mathbf{h}] \cdot \begin{bmatrix} X_m \\ F_s \end{bmatrix} \quad \text{Hybrid parameter matrix} \tag{3}$$

$$\begin{bmatrix} X_m \\ F_s \end{bmatrix} = [\mathbf{g}] \cdot \begin{bmatrix} F_m \\ X_s \end{bmatrix} \quad \text{Inverse of } \mathbf{h} \text{ matrix} \tag{4}$$

$$\begin{bmatrix} F_m \\ X_m \end{bmatrix} = [\mathbf{F}] \cdot \begin{bmatrix} X_s \\ F_s \end{bmatrix} \quad \text{Transmission matrix} \tag{5}$$

$$\begin{bmatrix} X_s \\ F_s \end{bmatrix} = [\mathbf{F}^*] \cdot \begin{bmatrix} F_m \\ X_m \end{bmatrix} \quad \text{Inverse of } \mathbf{F} \text{ matrix.} \tag{6}$$

Strictly speaking, impedances relate forces and velocities. In this paper, however, positions will be used instead of velocities, since there is not usually direct velocity measurement in a robot, but position sensors.

It is worth noting that whichever of the previous matrices is selected, all of the information or characterization of the teleoperated system will be contained within it. In fact, it is easy to obtain the expression of any entry of any of the six matrices in terms of the four entries of one of the rest. However, some entries of these matrices have useful and interesting physical interpretation, whereas others have little physical significance.

The most popular matrix for the analysis of teleoperated systems is the hybrid parameter matrix $\mathbf{h}$ [5], [6], [8], [9], whose entries are defined in (7) and (8).

$$\begin{bmatrix} F_m \\ X_s \end{bmatrix} = \begin{bmatrix} h_{11} & h_{12} \\ h_{21} & h_{22} \end{bmatrix} \begin{bmatrix} X_m \\ F_s \end{bmatrix} \tag{7}$$

$$h_{11} = \left.\frac{F_m}{X_m}\right|_{F_s=0} \quad h_{12} = \left.\frac{F_m}{F_s}\right|_{X_m=0}$$
$$h_{21} = \left.\frac{X_s}{X_m}\right|_{F_s=0} \quad h_{22} = \left.\frac{X_s}{F_s}\right|_{X_m=0}. \tag{8}$$

The mathematical exigency of perfect transparency (i.e., managing to transmit an impedance equal to that of the contacted environment) imposed in [5] leads to the ideal values of the hybrid parameters specified in (7). The same conclusions can be drawn from the physical interpretation of the four parameters as, for instance, [6], [8], [9] do.

In fact, according to the mathematical definitions of such parameters (8) h_{11} gives the **unconstrained movement impedance**—the equivalent inertia and damping that the operator feels moving the master robot if the slave is unconstrained—which is desired to be as low as possible; entry h_{21} is the transfer function of the **position tracking** during unconstrained motion—i.e., the ability of the slave robot to copy the position of the master robot—which should tend to unity (if no position scaling is desired) with infinite bandwidth. As for h_{12}, it is related to the **tracking of forces** in contact tasks. However, it is not a very meaningful tracking of forces because it is defined when the operator keeps the master steady against the forces that the slave encounters, which is quite an unnatural way of working. Finally, h_{22} is connected with position tracking during contact tasks. In this paper, $-h_{22}$ will be called **contact admittance** (the reason for the minus sign is that F_s is the force that the slave exerts on the environment instead of the opposite). It is a nonphysical admittance generated by the controller and added to that of the environment $(1/Z_e)$, as the expression of the transmitted impedance Z_t shows

$$Z_t \equiv \frac{F_m}{X_m} = h_{11} + \frac{h_{12}h_{21}}{1/Z_e + (-h_{22})}. \tag{9}$$

Thus, for any nonzero contact admittance hard surfaces will be felt as much softer and the slave's position will be sensitive to external forces.

III. Set of Parameters to Experimentally Evaluate the Performance of a Teleoperated System

From the theoretical point of view, the four hybrid parameters allow both tuning and comparison of teleoperation systems [6]. However, it is not so clear whether they are that appropriate for experimental characterization purposes. This section is devoted to studying which is the best selection of parameters to be acquired experimentally, and still fully characterize the teleoperated system. The easiest experiments with any teleoperated systems are always free movement and hard contact tests, and these will be the starting point to select the best set of parameters.

A. Unconstrained Movement Test

Unconstrained motion is the free movement of the slave robot, remote from any environment with which interaction can be established. Mathematically, this movement is expressed as $F_s = 0$. Consequently, h_{11} and h_{21} are concerned here.

For this kind of test the operator should hold the master robot and move it while the slave robot tries to track the described trajectories as efficiently as possible. It is a simple experiment that allows the data of X_m, F_m, and X_s to be acquired when F_s is null, since the slave robot does not come into contact with anything. These data can be analyzed in the frequency domain to obtain the transfer functions of h_{11} and h_{21}, i.e., the free motion impedance and the position tracking of the slave over the master, according to (8).

It can be seen, then, that unconstrained motion performance can be easily evaluated through a simple experiment that requires no extra preparation of the system. Therefore, the two parameters of the left column of the hybrid matrix $\mathbf{h}$ are worthy for both mathematical and experimental analysis, as they are meaningful and easy to measure. Unfortunately, the right column parameters do not offer this double advantage.

B. Hard Contact Test

As (8) show, h_{12} and h_{22} have to be obtained while the master robot is steady $(X_m = 0)$. So, the procedure to acquire the experimental data that allow the calculation of these transfer functions would be to fix the master manipulator and to apply forces onto the slave end-effector. Usually, however, it is physically difficult to guarantee that the master robot does not move at all, and even more if the measurement of the force to achieve so (F_m) is required. Second, slave manipulators can be extremely heavy in order to be able to exert very high forces onto the environment (macromanipulation) and so it is even more difficult to be able to handle it and provide the necessary forces to achieve quality measurements. Finally, it may also occur that the slave robot is nonaccessible for being in space, deep in water, in a radioactive environment, etc.

Furthermore, the physical significance of these parameters may be intuitively related to contact tasks but it would be much clearer and natural if the restriction were $X_s = 0$ instead of $X_m = 0$ (mainly the tracking of forces). In normal operation, achieving $X_s = 0$ is easier since it is merely making the slave robot contact a hard surface.

Accordingly, h_{12} and h_{22} are not so useful as elements of experimental validation, but rather as simple tuning references found within the hybrid parameter matrix $(\mathbf{h})$. So, another pair of parameters must be found which fulfill four basic requirements. They must characterize the behavior of the system in contact tasks, be physically meaningful and intuitive, be a complete set of parameters (any entry of the matrices (1) to (6) should be possible to obtain in terms of a function of them) and be obtainable by means of one simple experiment.

Where simplicity of testing is concerned, parameters associated with hard contact tasks are the most desirable, since they can be measured through ordinary teleoperation, with no extra elements or preparation of the system. So, the proposed pair of parameters is the following

$$Z_{11} = \left.\frac{F_m}{X_m}\right|_{X_s=0} \qquad F_{12} = \left.\frac{F_m}{F_s}\right|_{X_s=0}. \tag{10}$$

These data for X_m, F_m and F_s can be obtained by making the slave robot contact a very hard surface where penetration does not take place, so that $X_s = 0$ can be assumed. The first parameter Z_{11} is the **maximum transmittable impedance** for a particular architecture or system. Since the capability of the system to transmit impedance is not infinite, it will "saturate" beyond a certain value of the contacted impedance. Thus, it is desired that this parameter is as large as possible, as [10] thoroughly explains. The second parameter F_{12} gives the **tracking of forces in hard contact tasks** and is expressed in terms of the quotient of the force that the operator makes on the master and that force effectively exerted on the environment by the slave robot.

C. Completeness of the Selected Parameters

As a result of the exposed analysis, the most convenient set of parameters for the experimental validation of a teleoperated system consists of the four parameters proposed in Table I. This table shows also what matrix or matrices each parameter belongs to and where it is located inside those particular matrices.

Unfortunately, none of the available matrix representation options ((1) to (6)) includes all of them, but it appears clear that the matrices composed of hybrid parameters (trackings, impedances, and admittances) are more complete in terms of our analysis, with the exception of $\mathbf{F}^*$, which, in fact, is never used.

While any of the proposed matrices provides complete information or characterization of the teleoperated system, it is not so clear whether any arbitrarily chosen set of four parameters (picked from several matrices) will achieve the same. In fact, it will not in general, but fortunately this problem does not appear with the proposed set of parameters, namely h_{11}, h_{21}, Z_{11}, and F_{12}. This can be easily demonstrated.

If h_{11}, h_{21}, Z_{11}, and F_{12} formed a full-meaning set of parameters (i.e., if they were nonredundant and therefore no information were lost), then the four elements of any of the six matrices could be expressed in terms of these four parameters. The reader could easily obtain the next two expressions that construct h_{12} and h_{22} (the elements of the hybrid parameter matrix not selected for the proposed 4-parameter set) in terms of the chosen parameters

$$h_{12} = F_{12}\frac{Z_{11} - h_{11}}{Z_{11}} \quad h_{22} = -F_{12}\frac{h_{21}}{Z_{11}}. \tag{11}$$

As a result, it can be asserted that the proposed parameters convey all the characteristics of the teleoperated system and, furthermore, are very easy to obtain through the two simplest experiments.

IV. Application to Different Control Schemes

Traditionally, the classification of the different control architectures is made on the basis of the exchanged information between robots. This information can concern force or position and can travel from the master robot to the slave robot or the other way round. This gives four information channels available for the control scheme to rule the system.

A. PP Controller

As the name of this architecture suggests, the only information required is the position of the robots. In this way, the path of the master robot X_m is used as reference trajectory for the slave robot. This will try to follow it by means of a PD position controller $(\mathrm{PD_s} = K_s + sD_s)$, which acts like a spring of stiffness K_s and a damper of constant D_s. The whole control scheme is depicted in Fig. 1 and is totally symmetric, which means that the master robot also receives the position of the slave X_s as a reference trajectory. Force reflection is obtained as a result of the actuation produced by the $\mathrm{PD_m}$ controller when tracking error grows due to the interaction between the slave robot and the contacted environment (again, the analogy with the spring-damper set can be used).

The parameters shown in Fig. 1 will also be present in the remaining control schemes. In these, both robots are represented by their impedances (in terms of positions, not velocities), Z_m and Z_s (with subscript m always being used to refer to the

TABLE I
MATCHING BETWEEN THE SELECTED PARAMETERS AND THE ENTRIES OF THE DIFFERENT MATRICES. IN BRACKETS, DESIRED VALUES FOR NON-SCALED TELEOPERATION

	Z	Y	h	G	F	F*
$h_{11}=\left.\frac{F_m}{X_m}\right\|_{F_s=0}$ $(\to 0)$		$\frac{1}{Y_{11}}$	h_{11}			
$h_{21}=\left.\frac{X_s}{X_m}\right\|_{F_s=0}$ $(\to 1)$			h_{21}		$\frac{1}{F_{21}}$	
$F_{12}=\left.\frac{F_m}{F_s}\right\|_{X_s=0}$ $(\to 1)$				$\frac{1}{g_{21}}$	F_{12}	
$Z_{11}=\left.\frac{F_m}{X_m}\right\|_{X_s=0}$ $(\to \infty)$	Z_{11}			$\frac{1}{g_{11}}$		

master robot, and subscript s to the slave robot), which are established by means of the impedance controller presented in Section B. Thus, using the Laplace variable s

$$Z_{m,s} = M_{m,s}s^2 + B_{m,s}s. \tag{12}$$

Added to the control forces provided by $\mathrm{PD_m}$ and $\mathrm{PD_s}$. the schemes show a second force acting on the robots, due to the operator or to the environment, in the case of the master or the slave, respectively. Consider the case of operator–master interaction first. The operator must exert a force not only to move the master robot but also to move his/her own arm, so the total force τ_{op} is related to the force applied to the master f_m as follows:

$$\tau_{\mathrm{op}} = f_m + Z_{\mathrm{op}}X_m \tag{13}$$

where Z_{op} represents the impedance of the operator's arm. Similarly, we can express the external force that acts on the slave robot $-f_s$ as the sum of that resulting from its interaction with an environment of impedance Z_e and that directly applied to the slave by other external sources τ_e

$$-f_s = \tau_e + (-Z_eX_s). \tag{14}$$

Fig. 1 includes all these relationships so that the system, the operator and the environment are all taken into account. Study of the block diagram leads to the analytical expressions of the proposed 4-parameter set presented in Table II.

Several comments can be made about the expressions shown in Table II. First, it can be demonstrated [7] that if the system is linear and continuous, it will be stable for any gain of the PD controllers. Second, it is obvious that the larger the gains of the PD controllers, the better performance. So, assuming that the gains of the PD controllers will be large, some simplifications are made in Table II. These indicate, for instance, that the higher $\mathrm{PD_s}$ the better the tracking. Besides, if the force restitution is one to one $(F_{12}=1)$, then $\mathrm{PD_m}=\mathrm{PD_s}$ and so, the maximum transmittable impedance will be $\mathrm{PD_m}$, and the impedance in unconstrained movement the sum of the impedances of both robots.

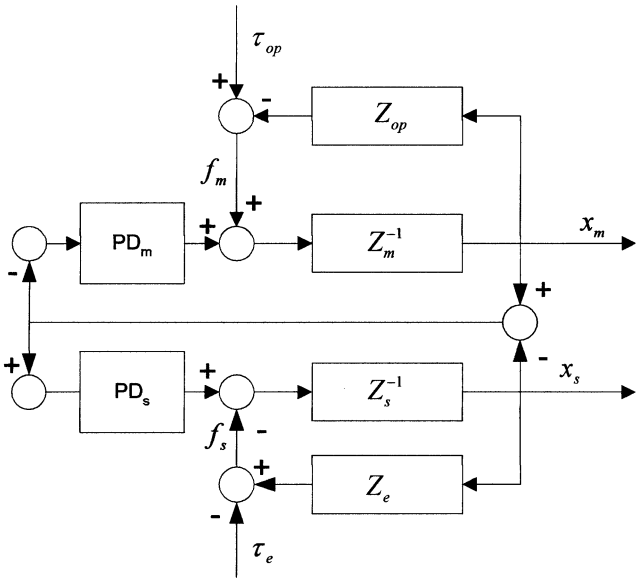

Fig. 1. Block diagram of a PP controller [7].

TABLE II
COMPLETE AND SIMPLIFIED ANALYTICAL EXPRESSIONS OF THE PROPOSED SET OF PARAMETERS FOR THE POSITION–POSITION CONTROL SCHEME

Unconstrained movement impedance	$h_{11} = Z_m + \frac{PD_m \cdot Z_s}{PD_s + Z_s} \approx Z_m + \frac{PD_m}{PD_s}Z_s$
Position tracking in free movement	$h_{21} = \frac{PD_s}{Z_s + PD_s} \approx 1$
Force tracking in hard contact tasks	$F_{12} = \frac{Z_m + PD_m}{PD_s} \approx \frac{PD_m}{PD_s}$
Maximum Transmittable impedance	$Z_{11} = Z_m + PD_m \approx PD_m$

B. FP Controller

This controller is perhaps the most intuitive of all. As shown in Fig. 2, the control scheme corresponding to the slave robot is identical to that of the PP controller, so the slave robot is dedicated to following the trajectory of the master by means of $\mathrm{PD_s}$. When the environment is contacted, the forces that appear on the slave must be measured and generated on the master so that the operator can feel them, scaled by constant K. Therefore, this control scheme requires a force sensor to be installed on the wrist of the slave.

The analytical expressions for the proposed four-parameter set are given in Table III and can be easily obtained from the equations that the block diagram represents. With this controller, it can be demonstrated that the system is stable for any environment [1], [7] if K is less than a critical value. This value is roughly the quotient of the masses of the master and the slave robots. In fact, the main limitation of this architecture concerns stability, the study of which is beyond the scope of this paper. A notch filter can be used in the force channel instead of constant gain (K) to improve the stability of the control system [1]. Other authors [11] propose to modify the position channel with a

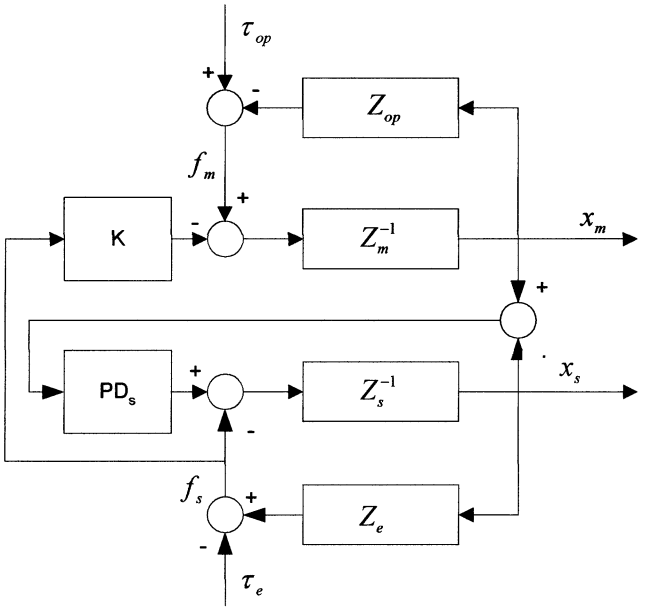

Fig. 2. Block diagram of a FP controller [7].

loop-shaping filter and include local force feedback loops. However, the aim of the authors is not to optimize the control architectures but just to show the validity of the proposed parameters to assess them, and that is why a simple proportional force reflection will be used in this teleoperation algorithm.

C. 4C Controller

The 4C architecture makes use of all the information that the teleoperated system generates. It thus requires position and force sensors in both robots in order to feed data to the four communication channels depicted in Fig. 3 (C_1, C_2, C_3, and C_4). An extension of this control scheme can be seen in [5], where local force feedback loops are included.

In this algorithm, all the parameters are very coupled and it is not easy to predict how a change in any of them will affect the performance of the system. However, the analytical expressions obtained for this control scheme (Table IV) show its capability to achieve perfect transparency by tuning the transfer functions of the different communication channels as follows [3]:

$$\begin{aligned} C_1 &= Z_s + C_s \quad C_2 = 1 \\ C_4 &= -(Z_m + C_m) \quad C_3 = 1 \end{aligned} \tag{15}$$

The tuning given by (15) leads to null unconstrained movement impedance, unitary force and position tracking with infinite bandwidth and also unlimited maximum transmittable impedance. Unfortunately, this selection of parameters needs the evaluation of accelerations. Lawrence proposes [3], in practical applications, to include only velocity terms in the C_1 and C_4 transfer functions, which eliminates the possibility of null unconstrained movement impedance.

TABLE III
ANALYTICAL EXPRESSIONS OF THE PROPOSED SET OF PARAMETERS FOR THE FORCE-POSITION CONTROL SCHEME

Unconstrained movement impedance	$h_{11} = Z_m$
Position tracking during unconstrained movement	$h_{21} = \dfrac{PD_s}{Z_s + PD_s}$
Force tracking in hard contact tasks	$F_{12} = K + \dfrac{Z_m}{PD_s}$
Maximum Transmittable impedance	$Z_{11} = Z_m + KPD_s$

V. DESCRIPTION OF THE PHYSICAL SYSTEM

A. Hardware Structure of the System

The 2-DOF master–slave system shown in Fig. 4 has been used [12]. Four conventional dc motors driven by power amplifiers, configured as current sources, actuate the two pantograph mechanisms used as master and slave devices. A computer rules the whole system, on the basis of the running algorithm and the data received from the encoders and force sensors through a data acquisition board.

Given that in previous experiments performed by the authors [13], the pulley-belt transmission showed itself to be very effective, the effects of friction will be neglected. Therefore, the dynamics of the robots is given by the following expression

$$\boldsymbol{\tau} + \mathbf{J}^{\mathbf{T}}\mathbf{f}_{\text{ext}} = \mathbf{M}(\mathbf{q})\ddot{\mathbf{q}} + \mathbf{V}(\mathbf{q}, \dot{\mathbf{q}}) \tag{16}$$

where $\mathbf{M}$ is the inertia matrix, $\mathbf{V}$ contains the centripetal and Coriolis terms, $\mathbf{J}$ is the Jacobian matrix of the manipulator, $\boldsymbol{\tau}$ is the torque exerted by the robot actuators, and $\mathbf{f}_{\text{ext}}$ is the force that the operator or the environment exert on the master or slave robot, respectively.

B. Impedance Controller

A precise knowledge of the values of the dynamic parameters of the system allows the implementation of an inverse dynamics algorithm as impedance controller, converting the behavior of the robots to that of a mass immersed in a viscous environment, as assumed in (12). Thus, the torque given by the motors can be split into two terms, the first arising from the teleoperation $\boldsymbol{\tau}_{\text{Tel}}$, and the second, from the impedance control $\boldsymbol{\tau}_{\text{InvDyn}}$, so that

$$\boldsymbol{\tau} = \boldsymbol{\tau}_{\text{Invdyn}} + \boldsymbol{\tau}_{\text{Tel}} = \boldsymbol{\tau}_{\text{Invdyn}} + \mathbf{J}^{\mathbf{T}}\mathbf{f}_{\text{Tel}}. \tag{17}$$

If m and b are the desired mass and damping and $\mathbf{z}$ is a vector containing the Cartesian coordinates, the target relationship between the movement of each robot and the forces that act on it will be as follows [14]:

$$\mathbf{f}_{\text{ext}} + \mathbf{f}_{\text{Tel}} = m\ddot{\mathbf{z}} + b\dot{\mathbf{z}}. \tag{18}$$

Considering that position sensors measure manipulator coordinate $\mathbf{q}$, Cartesian coordinates must be related to the former, and also their derivatives through the Jacobian matrix

$$\mathbf{z} = \mathbf{h}(\mathbf{q}) \rightarrow \dot{\mathbf{z}} = \mathbf{J}\dot{\mathbf{q}} \rightarrow \ddot{\mathbf{z}} = \dot{\mathbf{J}}\dot{\mathbf{q}} + \mathbf{J}\ddot{\mathbf{q}}. \tag{19}$$

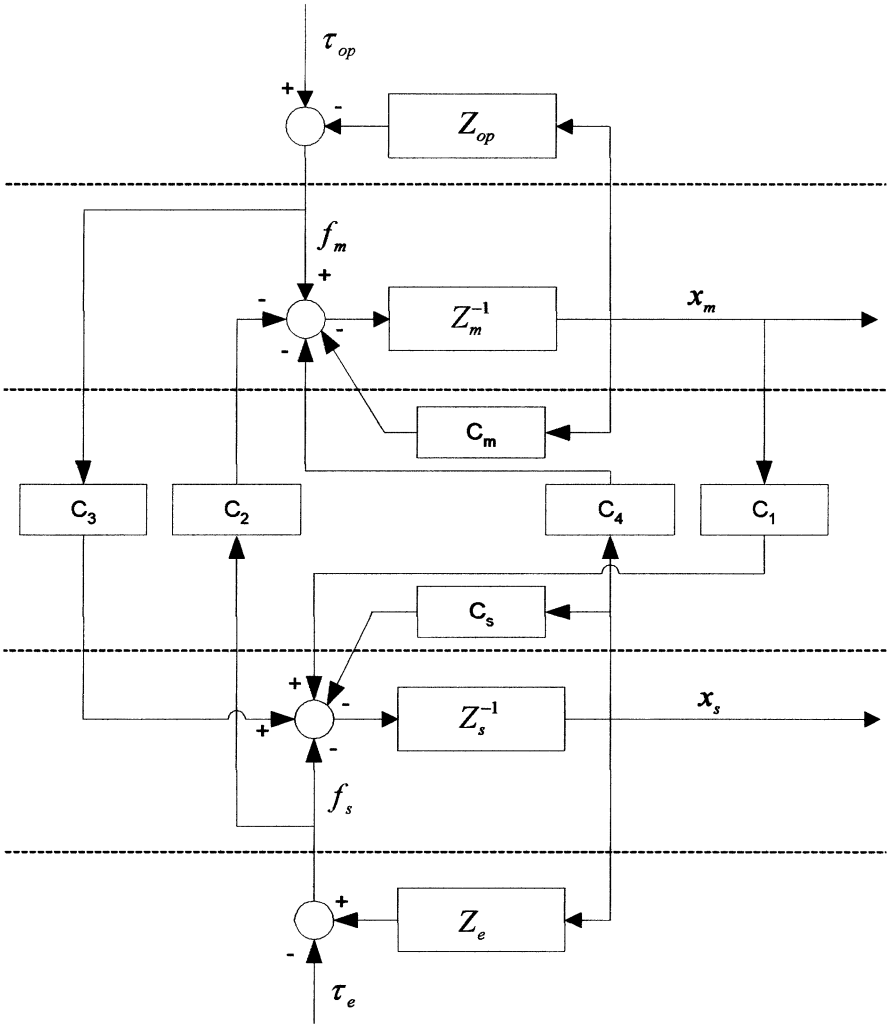

Fig. 3. Block diagram of the 4C controller [3].

TABLE IV
ANALYTICAL EXPRESSIONS OF THE PROPOSED SET OF PARAMETERS FOR THE FOUR-CHANNEL ARCHITECTURE

Unconstrained movement impedance	$h_{11}=\dfrac{(Z_m+C_m)(Z_s+C_s)+C_1C_4}{(Z_s+C_s)-C_3C_4}$
Position tracking during unconstrained movement	$h_{21}=\dfrac{C_1+C_3(Z_m+C_m)}{(Z_s+C_s)-C_3C_4}$
Force tracking in hard contact tasks	$F_{12}=\dfrac{(Z_m+C_m)+C_1C_2}{(Z_m+C_m)C_3+C_1}$
Maximum Transmittable impedance	$Z_{11}=\dfrac{(Z_m+C_m)+C_1C_2}{1-C_2C_3}$

Substituting (19) in (18) and operating, the acceleration that the system experiences is as follows:

$$\ddot{\mathbf{q}} = m^{-1}\mathbf{J}^{-1}(\mathbf{f}_{\text{ext}} + \mathbf{f}_{\text{Tel}} - b\mathbf{J}\dot{\mathbf{q}} - m\dot{\mathbf{J}}\dot{\mathbf{q}}). \tag{20}$$

Substituting (20) into (16), leads to the torques that must be applied to the robots together with those arising from teleoperation, $\boldsymbol{\tau}_{\text{Tel}}$ (17), in order to obtain the behavior of a mass plus a damper; and therefore, linear and decoupled.

$$\boldsymbol{\tau}_{\text{InvDyn}} = \frac{1}{m}\mathbf{M}(\mathbf{q})\mathbf{J}^{-1}(\mathbf{f}_{\text{ext}} + \mathbf{f}_{\text{Tel}}) - \frac{b}{m}\mathbf{M}(\mathbf{q})\dot{\mathbf{q}} - \mathbf{M}(\mathbf{q})\mathbf{J}^{-1}\dot{\mathbf{J}}\dot{\mathbf{q}} + \mathbf{V}(\mathbf{q},\dot{\mathbf{q}}) - \mathbf{J}^{\mathbf{T}}(\mathbf{f}_{\text{ext}} + \mathbf{f}_{\text{Tel}}). \tag{21}$$

VI. COMPARISON OF EXPERIMENTAL RESULTS

A. Tuning of the Control Schemes

The same unconstrained motion impedance for all three controllers was established, so that the operator would not feel any differences in terms of fatigue while operating the system in unconstrained motion. The authors think that this permits a fair comparison between the three algorithms. This impedance was set to the following

$$h_{11} = 0.4s^2 + 0.8s. \tag{22}$$

Considering the **position-position** controller (PP), free motion impedance (see Table II) is given by

$$h_{11\text{PP}} = Z_m + \frac{\text{PD}_m}{\text{PD}_s + Z_s}Z_s$$

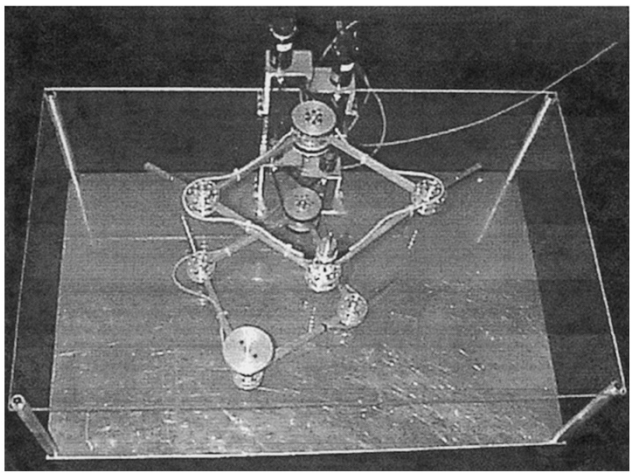

Fig. 4. Photography of the arrangement of the master and slave robots.

$$\approx Z_m + \frac{\mathrm{PD}_m}{\mathrm{PD}_s} Z_s \approx Z_m + F_{12} Z_s. \tag{23}$$

Equation (23) shows one of the main problems of the PP architecture: unconstrained motion impedance is always that of the master robot increased by a certain proportion of the slave impedance, which is usually much heavier. Since low impedance is desired for free movement, the target impedances for both robots should be low, which tends to make the inverse dynamics algorithm unstable. The smallest achievable impedances that guarantee this stability in any conditions were determined experimentally and are as follows:

$$\begin{aligned} Z_m &= 0.15s^2 + 0.30s \\ Z_s &= 0.60s^2 + 1.20s. \end{aligned} \tag{24}$$

As it is necessary that (22) holds, substituting (24) in (23) gives the following

$$\mathrm{PD}_m = 0.417 \mathrm{PD}_s. \tag{25}$$

As a result, the only parameters that can be tuned for optimum performance are the proportional and derivative constants of $\mathrm{PD_s}$ (see Fig. 1). These will be set at the highest possible values that keep the system stable, since all the parameters shown in Table II take advantage of this. Given $\mathrm{PD_s} = K_s + D_s \cdot \mathrm{s}$, K_s is assigned a value of 1550 N/m and D_s, 61 Ns/m.

It is important to notice that the requirements of stability of the inverse dynamics control and low free motion impedance lead to a value of 0.417 for $\mathrm{PD_m/PD_s}$ (25), which approximately equals F_{12}. As a result, the only chance for a PP controller to achieve a larger force transmission rate is by establishing larger impedance in free motion, as (23) shows. However, this solution is inappropriate because it is tiring for the operator and so, the forces presented to him must be scaled down.

The **force-position** controller (FP) presents a stability problem. As was stated before, roughly speaking, the force-scaling factor (K in Fig. 2) must be smaller than the quotient of the impedances of the master and slave robots [1], [7]. Taking into account (22) and the expression of the free motion impedance (Table III), the selected master impedance was

$$Z_m = 0.4s^2 + 0.8s. \tag{26}$$

Since it is desirable to keep K as close to one as possible, the slave impedance has to be similar to that of the master. However, respecting the stability limitation of the inverse dynamics given in (24) and choosing such Z_s, the largest value of K that yields a stable system has been

$$K = 0.62. \tag{27}$$

This experimental value is close to the quotient of Z_m and Z_s. It can be seen that in this case, the FP scheme achieves larger stable force reflection than the PP scheme.

For the **four-channel controller** (4C), the tuning was carried out through a very different path. In fact, its transfer functions (see Table IV) are much richer, in the sense that, unlike the previous architectures, they do allow theoretical tuning for perfect transparency to be achieved. This can be checked simply by choosing $C_2 = C_3 = 1$, so that infinite maximum transmittable impedance is achieved, as well as unitary force tracking with unlimited bandwidth. Although local force feedback as proposed in [5] were tried, the results were good enough without using them. Ideal results could also be achieved in free motion if C_1 and C_4 were tuned as (15) claim; but that implies the necessity of good signals for the accelerations of the robots, which are very difficult to get with encoders. So, the coefficients of s^2 in C_1 and C_4 were set to zero in order to avoid using noisy signals (resulting from double derivation of the encoders signals).

As a result of this simplification, the objective of free motion impedance given by (22) becomes impossible to attain according to the expression in Table IV. The most satisfactory solution was to decrease the desired impedance for free motion to $h_{11} = 0.4s^2$. The following tuning fulfills the previous conditions and, in addition, provides—theoretically—infinite bandwidth for unconstrained motion position tracking (h_{21})

$$\begin{aligned} M_m &= 0.4\,\mathrm{kg}, \quad M_s = 0.4\,\mathrm{kg} \\ B_m &= 5\,\mathrm{Ns/m}, \quad B_s = 40\,\mathrm{Ns/m} \\ C_m &= 1000\,\mathrm{N/m}, \quad C_s = 900\,\mathrm{N/m} \\ C_4 &= 5s + 1000, \quad C_1 = 40s + 900. \end{aligned} \tag{28}$$

B. Experimental Results

Each proposed parameter of the set will be analyzed to establish a quantitative comparison of the three tested algorithms on the basis of experimental measurements.

1) Free Motion Impedance (h_{11}): As Fig. 5 shows, the computed torque algorithm provided good control of the impedance in the range of frequencies below 50 rad/s, in which the experimental impedance is between 0, 5 and 0, 6 kg for PP and 4C controllers and between 0, 4 and 0, 5 kg in the case of the FP algorithm. The better accuracy obtained in the latter with respect to the desired $\mathrm{h_{11}}$ (22) is due to the fact that the FP controller is the only one in which the impedance of the slave has no influence on $\mathrm{h_{11}}$. In fact, the main sources of error in $\mathrm{h_{11}}$

are the inaccuracies of the impedance controllers of the robots. A more detailed analysis showed that the computed torque controller provided impedances with discrepancies of 0.05 to 0.1 kg between the real and the desired impedance due to unmodeled elements like the signal cables or the little friction of the system. These discrepancies appear in the experimental measurements of h_{11} as well, but only those connected with the master in the particular case of the FP controller.

2) Position Tracking in Free Motion (h_{21})*:* Fig. 6 shows a comparative Bode amplitude diagram of the three architectures in which the superiority of the 4C controller is clear. As for PP and FP architectures, their theoretical expressions of h_{21} are identical because the control over the slave robot follows the same rule. However, the curve for PP architecture differs significantly from that of FP architecture beyond 30 rad/s. This is because the estimation of the master velocity for high frequency was made dividing F_m and Z_m/s in the PP architecture, in order to reduce the noise resulting from the derivation of the position signal of the encoders, whose resolution was 6 time less than the slave's. This permitted to use higher values of the proportional and derivative constants of $\mathrm{PD_s}$ keeping he system stable, but it produced worse behavior at frequencies beyond 30 rad/s, as a simple comparison with the curve of the FP controller evidences.

So, if we compare the FP and 4C architectures, the latter appears clearly better in any sense

- At low frequency the gain of the tracking (X_s/X_m) is 0 dB, whereas in the case of FP it is about 0.6 dB.
- The growing of the gain toward the peak of resonance starts at the late frequency of 20 rad/s, while in the FP controller it occurs at only 10 rad/s.
- The peak of resonance is 2.5 dB at 50 rad/s in the 4C architecture and 3.5 dB at 30 rad/s in the FP controller. As a result, together with the previous points, the FP architecture amplifies any movement of the master in a higher proportion than the 4C does.
- The bandwidth of the 4C controller is about 70 rad/s, while the FP architecture provides only 62 rad/s.

This global superiority is even more noticeable when one actually operates a 4C controller after a test with the others; but the strength of this analysis lies in the fact that the objective parameters corroborate and quantify the subjective sensation of the operator.

3) Force Tracking in Hard Contact Tasks (F_{12})*:* The first conclusion that can be drawn from the analysis of Fig. 7 is that there are clear differences between high and low frequencies. In fact, in high frequencies there seems not to be differences between the controllers, while in lower frequencies the 4C architecture gives 0 db force gain up to near 10 rad/s. Due to the limitations of the other architectures they were unable to achieve such performance with stability, unless heavy impedances were used in free motion. Even though, the curves for PP an FP in the low frequency range are quite similar to those calculated theoretically.

4) Maximum Transmittable Impedance (Z_{11})*:* As Fig. 8 demonstrates, the 4C controller provides the largest transmittable impedance (eight times greater than the other two schemes) and once again all three curves mix in the region of high frequencies of the diagram. Regarding the PP and FP

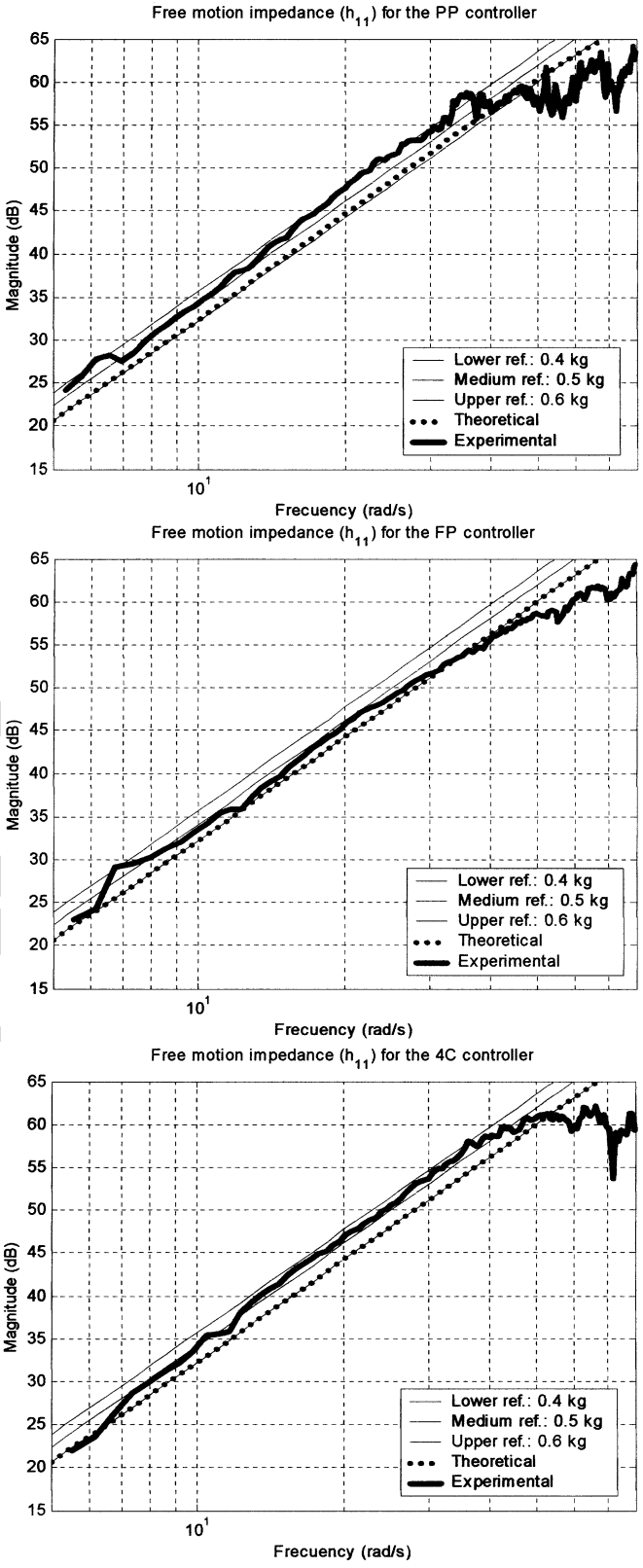

Fig. 5. Bode magnitude diagrams of the free movement impedance for PP, FP, and 4C architectures, including experimental results, theoretical predictions according to the expressions of h_{11} and reference curves $0.4s^2, 0.5s^2$ (medium), and $0.6s^2$ (uppermost).

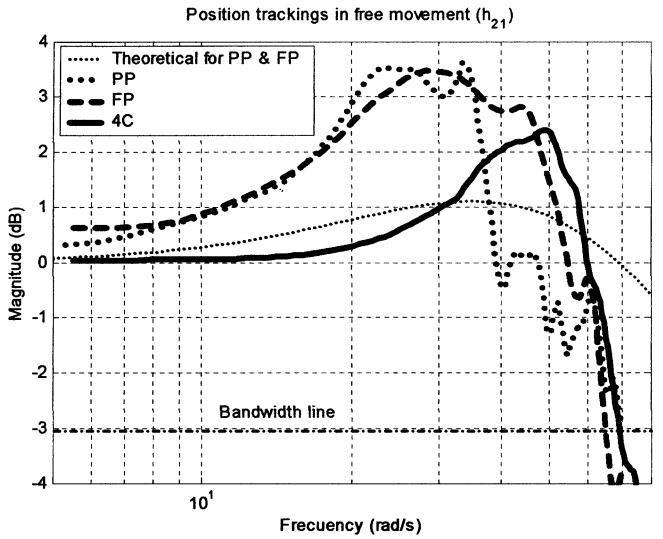

Fig. 6. Bode magnitude diagrams of the position trackings in free movement for PP, FP, and 4C architectures, including experimental results (smoothed for clarity) and theoretical predictions according to the expressions of h_{21}.

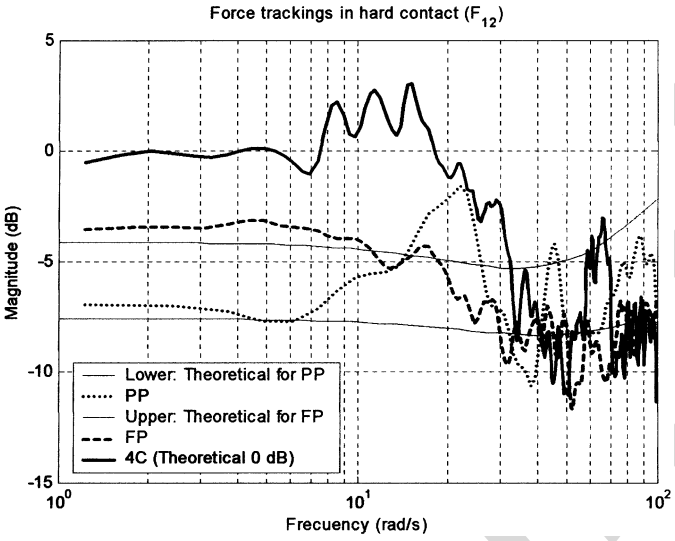

Fig. 7. Bode magnitude diagrams of the force trackings in hard contact for PP, FP, and 4C architectures, including experimental results (smoothed for clarity) and theoretical predictions according to the expressions of F_{12}.

architectures, both present similar experimental maximum transmittable impedances, and very close to those theoretically predicted.

C. Discussion

From this comparison, it can be seen that if there are force sensors in both robots, the 4C architecture outperforms any of the other two in any respect, be it position tracking, force tracking, force reflecting ratio or maximum transmittable impedance.

The great benefit of the PP architecture is that force sensors are not needed and that it is intrinsically stable. However, the large unconstrained movement impedance makes this architecture useful only if a very low force reflection ratio is needed.

The FP architecture is intermediate between the other two. The presence of a force sensor in the slave robot permits the

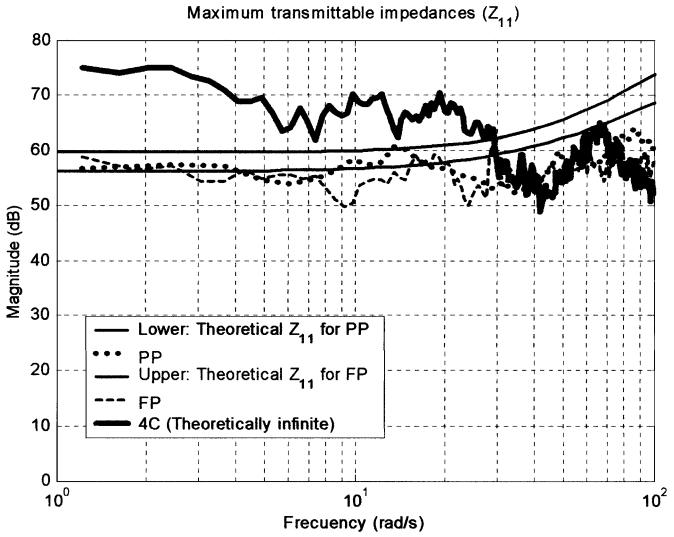

Fig. 8. Bode magnitude diagrams of the maximum transmittable impedances for PP, FP, and 4C architectures, including experimental results and theoretical predictions according to the expressions of Z_{11}.

implementation of an inverse dynamics impedance controller to decrease the apparent inertia of the robot and hence to increase the force reflection ratio.

VII. Conclusion

Theoretical support has been offered for a rigorous selection of parameters that allow the researcher to objectively/quantitatively evaluate the performance of a teleoperated system. A four-parameter set has been proposed that can be experimentally obtained through simple testing, measurement and further analysis in the frequency domain. The proposed method has been demonstrated in a 2 DOF test-bed equipped with position and force sensors and run under three different teleoperation algorithms: PP, FP, and 4C architectures. The transfer functions of all four parameter have been shown for the three architectures, regarding one of the degrees of freedom. The analysis of the second degree of freedom leads to analogous results.

The four parameters presented have shown themselves to be effective in the quantitative comparison of different teleoperation systems. The most novel parameter to evaluate experimentally may be the maximum transmittable impedance, Z_{11}. This parameter quantifies the stiffness of the contact in the teleoperation system and it is obtained via a simple hard contact experiment. This represents a significant advantage with respect the more traditionally used contact admittance h_{22}, since no direct excitation of huge slave robots nor complicated clamping of the master are required.

The most significant advantage of the PP controller has proved to be its stability; but in the context of industrial teleoperation (light masters and heavy slaves) it is unable to offer both large force-reflection ratios and light maneouvering capability. The FP architecture outperforms the force reflection ratio of the PP architecture, and slightly larger transmittable impedances have been obtained. Force measurements are used more efficiently in this scheme than in the PP architecture.

The 4C controller allows optimal employment of the information that the system generates in order to achieve very good performance not only in free motion but also in contact tasks, proving to be clearly superior to the other algorithms from any point of view.

REFERENCES

[1] R. W. Daniel and P. R. McAree, "Fundamental limits of performance for force reflecting teleoperation," *The Int. J. Robot. Res.*, vol. 17, no. 8, pp. 811–830, Aug. 1998.

[2] L. F. Peñín, K. Matsumoto, and S. Wakabayashi, "Force reflection for time-delayed teleoperation of space robots," *Proc. 2000 IEEE Int. Conf. Robot. Automation*, vol. 4, pp. 3120–3125, Apr. 2000.

[3] D. A. Lawrence, "Stability and transparency in bilateral teleoperation," *IEEE Trans. Robot. Automat.*, vol. 9, pp. 624–637, Oct. 1993.

[4] Y. Yokokohji and T. Yoshikawa, "Bilateral control of master-slave manipulators for ideal kinesthetic coupling. Formulation and experiment," *IEEE Trans. Robot. Automat.*, vol. 10, pp. 605–620, Oct. 1994.

[5] K. Hashtrudi-Zaad and S. E. Salcudean, "On the use of local force feedback for transparent teleoperation," *Proc. 1999 IEEE Int. Conf. Robot. Automat.*, vol. 3, pp. 1863–1869, May 1999.

[6] B. Hannaford, "A design framework for teleoperators with kinesthetic feedback," *IEEE Trans. Robot. Automat.*, vol. 5, pp. 426–434, Aug. 1989.

[7] L. F. Peñín, "Bilateral control of teleoperated robots. Contributions in force refection," Ph.D. dissertation, Madrid, 1998. in Spanish.

[8] B. Hannaford, "Stability and performance tradeoffs in bi-lateral telemanipulation," *Proc. 1989 IEEE Int. Conf. Robot. Automat.*, vol. 3, pp. 1764–1767, 1989.

[9] H. Flemmer, B. Eriksson, and J. Wikander, "Control design and stability analysis of a surgical teleoperator," *Mechatronics*, vol. 9, pp. 843–866, 1999.

[10] J. E. Colgate and J. M. Brown, "Factors affecting the Z-width of a haptic display," *Proc. 1994 IEEE Int. Conf. Robot. Automat.*, vol. 4, pp. 3205–3210, May 1994.

[11] K. B. Fite, J. E. Speich, and M. Goldfarb, "Transparency and stability robustness in two-channel bilateral telemanipulation," *ASME J. Dynam. Syst., Measure. Contr.*, vol. 123, no. 3, pp. 400–407.

[12] A. Rubio, A. Avello, and J. Florez, "Adaptive impedance modification of a master-slave manipulator," *Proc. 1999 IEEE Int. Conf. Robot. Automat.*, vol. 3, pp. 1794–1799, May 1999.

[13] I. Aliaga, "Implementation and comparison of several force-reflecting teleoperation architectures, in a 2 D.O.F. master-slave system," Master Thesis, Dec. 2000. in Spanish.

[14] N. Hogan, "Impedance control: An approach to manipulation. Part I—Theory," *J. Dynam. Syst., Measure. Contr.*, vol. 107, pp. 1–7, Mar. 1985.

Iñaki Aliaga was a researcher with the Centro de Estudios e Investigaciones Técnicas de Gipuzkoa (CEIT), Spain. He is now the Engineering Manager and cofounding partner of LANDER Simulation and Training Solutions, S.A. He is an industrial engineer (awarded Best Spanish National Graduate) with a wide investigation profile. He has developed projects of research for several departments of CEIT, such as the design and calculation of structures by means of finite element methods or R&D projects about the different architectures of force reflecting teleoperation. He is experienced in network communications and software development. Since 2002, his research is focused on simulation technologies, around which he is preparing work for the Ph.D. degree.

Ángel Rubio received the Master's degree in electrical engineering from the Politechnical University, Madrid, Spain, in 1994, and the Ph.D. degree from the Universidad de Navarra (TECNUN), Spain, in 1999.

His research interests include robotics, virtual reality, haptics, simulators, and control engineering. He is currently a researcher with Centro de Estudios e Investigaciones Técnicas de Gipuzkoa (CEIT), Spain, and an Associate Professor of control engineering and signals and systems from the Universidad de Navarra.

Emilio Sánchez received the Ph.D. degree in electrical engineering from the Universidad de Navarra (TECNUN), Spain, in 2002.

His research interests include teleoperation, mobile robotics, simulators, haptics, noise analysis, and control engineering. He is currently a researcher with Centro de Estudios e Investigaciones Técnicas de Gipuzkoa (CEIT), Spain, and a lecturer with the Universidad de Navarra.